Supplementary Material for Photodissociation of *iso*-Propoxy (*i*-C_3H_7O) Radical at 248 nm

Erin N. Sullivan, Steven Saric and Daniel M. Neumark[1]

Department of Chemistry, University of California, Berkeley, California 94720, USA and Chemical Sciences Division, Lawrence Berkeley National Laboratory, Berkeley, California 94720, USA

Simulations:

Figure S1 presents the comparison of simulated and experimental mass distributions. The simulated distributions are generated using the translational energy distribution of the included channels. For a given $E_{T,}$ the arrival time and positions of two fragments can be determined. By doing this for a large sample of events, the mass distributions can be simulated and the intensities adjusted to match that of the experimental distribution.

Similar to the fitted mass simulations, translational energy distributions can be used to examine the effect of false coincidences in the experimental results, as is done in Figure S2. The translational energy distribution is used to generate a sample of events from channel 1 or 5. These events are detected with a one-particle detection efficiency of 0.6. If a third fragment or particle hits the detector and is simulated to be detected with a high efficiency, then the event is assigned as three-body channel. The most likely assignment to that third particle is an H atom. The simulated translational energy distribution for this "false" three-body channel is similar to that for channel 11, thereby suggesting that channel 11 is not a true three-body channel.

[1] Corresponding author. Email: dneumark@berkeley.edu

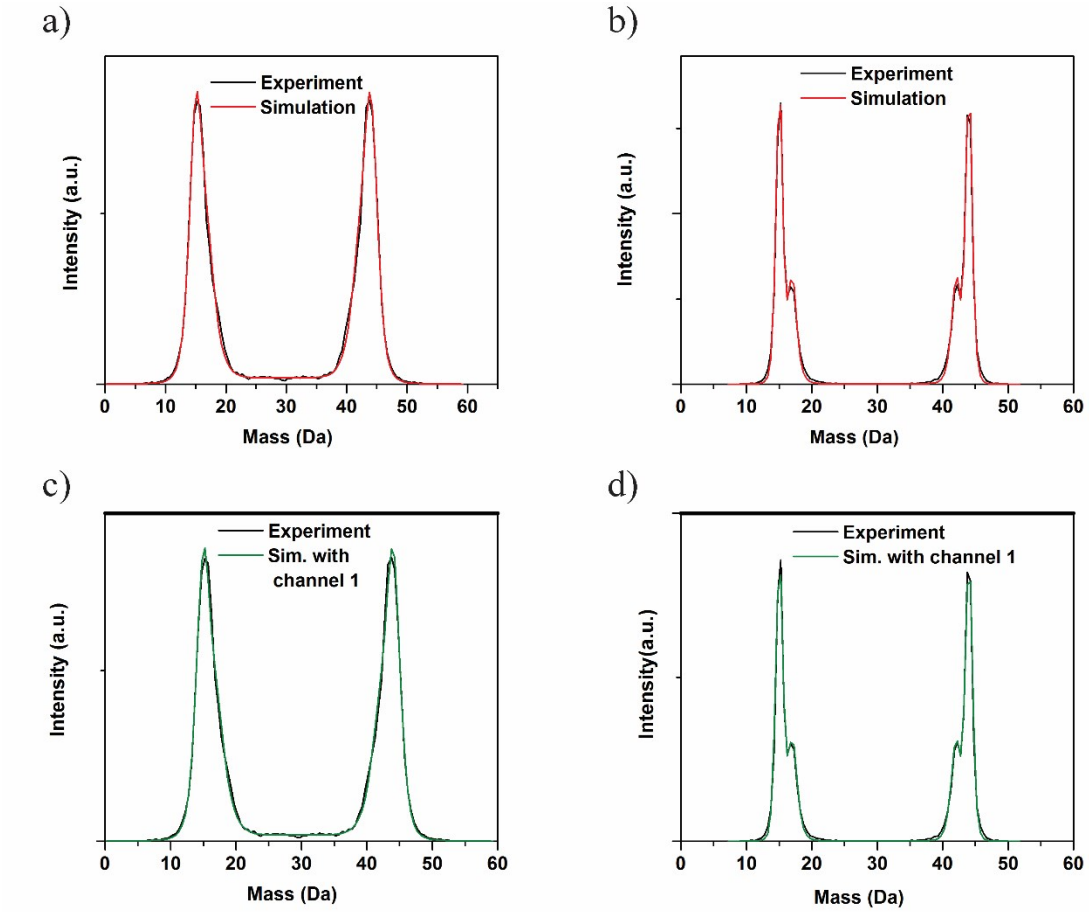

Figure S1: Experimental and simulated mass distributions. Panels a and b present the fitted mass distributions in red assuming the presence of channels 1 (CH_3 + CH_3CHO) and 5 (OH + C_3H_6) for the results using λ_{detach} = 532 nm and 655 nm, respectively. Panels c and d present the fitted distributions assuming that channel 8 (O + C_3H_7) is an additional channel, again at both detachment wavelengths. In the latter distributions, the best fit was found when the contribution of channel 8 was 0%, thereby confirming our analysis that channels 1 and 5 are the predominant two-body dissociation channels.

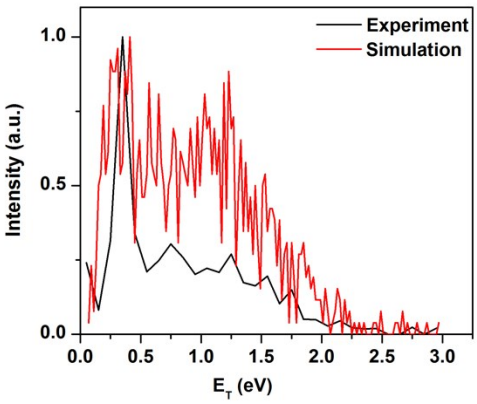

Figure S2: Comparison of the experimental translational energy distribution for the formation of channel 11 ($CH_3 + H + C_2H_3O$) and a simulated distribution in which an additional particle hitting the detector is assigned to a three-body event involving H loss.

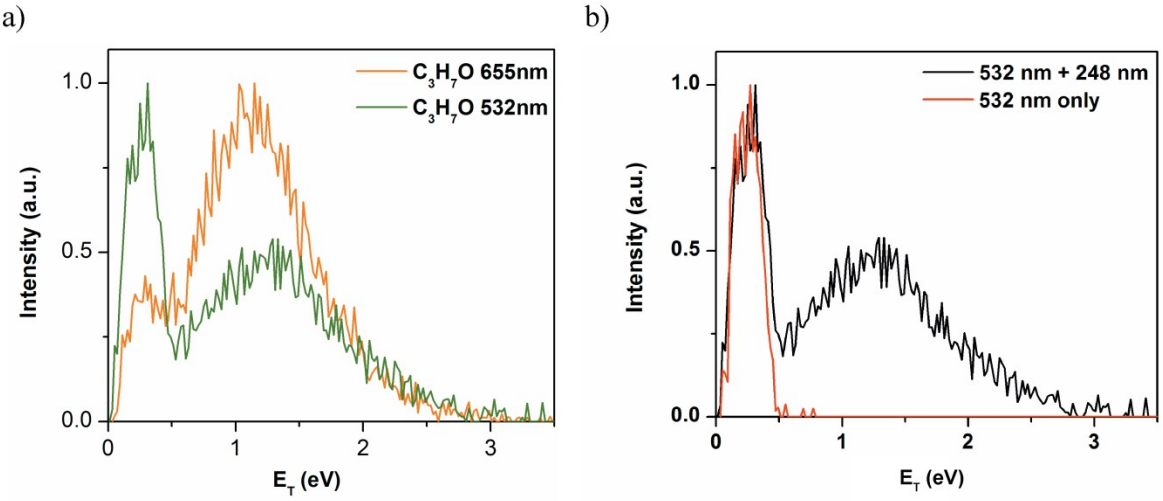

Figure S3: Panel a presents a comparison of translational energy distributions for dissociation of *i*-C_3H_7O to channel 1 ($CH_3 + CH_3CHO$) using different detachment wavelengths to generate the initial *i*-C_3H_7O radical. 655 nm (1.89 eV) detachment wavelength is shown in orange and is just above the electron affinity of the neutral radical. 532 nm (2.33 eV) detachment wavelength is shown in green. Panel b presents the translational energy distributions for experiments performed using 532 nm as the detachment wavelength and 248 nm as the dissociation wavelength (shown in black) and with only the detachment laser on (shown in red). These experiments demonstrate the dissociation of *i*-C_3H_7O from just the 532 nm detachment laser.

Newton Diagrams:

To better understand the mechanism by which channels 9 ($CH_3 + CH_4 + CO$) and 10 ($CH_3 + CH_3 + HCO$) fall apart, Newton diagrams have been plotted for each channel in Fig. S4.[1] The momentum vectors of the three photoproducts are mapped in the center of mass frame. The CH_3 fragment momentum vector is set to +1 in the positive direction as shown by the orange arrow. The momentum vectors of the other two fragments are normalized relative to this and plotted in the +y and -y directions. The classification of three-body dissociation events as synchronous

concerted, asynchronous concerted, or sequential[2] can be further examined using these plots. A sequential mechanism would manifest as a circle of intensity symmetric about the -x-axis that represents the momentum imparted to CO and CH_4 (channel 9) or HCO and CH_3 (channel 10). Following the dissociation of CH_3CHO into C_2H_4O and CH_3, C_2H_4O can dissociate into the remaining fragments after some time delay such that the momentum vectors are mapped in a circle. As there is no clearly defined circle in either plot, a sequential mechanism is not the appropriate classification for these three-body decay processes. Thus, in coordination with the Dalitz plots of Fig. 6 in the main text, an asynchronous concerted mechanism is the most appropriate.

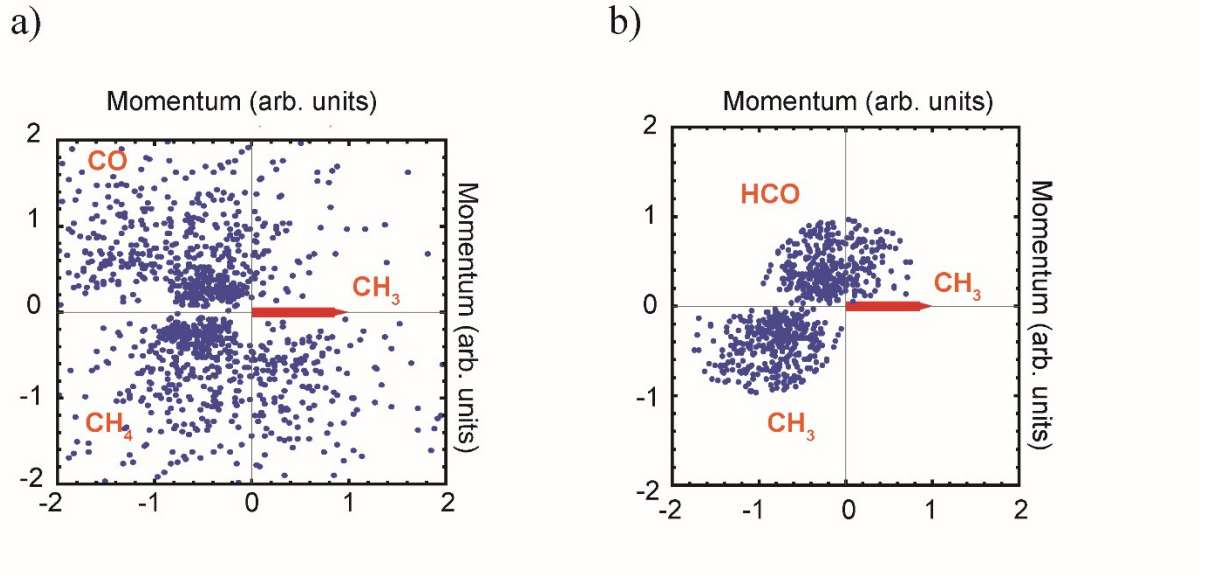

Figure S4: Newton diagrams for the three-body dissociation of *i*-C_3H_7O into channel 9 (CH_3 + CH_4 + CO) (panel a) and channel 10 (CH_3 + CH_3 + HCO) (panel b).

References:

1. N. Neumann, D. Hant, L. P. Schmidt, J. Titze, T. Jahnke, A. Czasch, M. S. Schoffler, K. Kreidi, O. Jagutzki, H. Schmidt-Böcking, and R. Dörner, *Phys. Rev. Lett.* 2010, **104**, 103201.
2. C. Maul and K.-H. Gericke, *Inter. Rev. Phys. Chem.,* 1997, **16**, 1-79.